Measured on Brusa

Department:	Research and Innovation Centre for Electrical Engineering
Research report no.:	22190-011-2021
Report type:	Research report
Authors:	Ondřej Suchý, Štěpán Janouš, Jan Laksar
Project leader:	Zdeněk Peroutka
Pages:	18
Release date:	8. 3. 2021
CEP Classification:	2.2 Electrical engineering, Electronic engineering, Information engineering - Electrical and electronic engineering

Customer:

Supplier:

University of West Bohemia in Pilsen
Research and Innovation Centre
for Electrical Engineering
Univerzitní 8
306 14 Plzeň

Contact person:

Ondřej Suchý
tel. +420377634949
suchyo@fel.zcu.cz

This research has been realized using the support of Technological Agency, Czech Republic, programme National Competence Centres, project # TN01000026 Josef Bozek National Center of Competence for Surface Vehicles.

Abstract

This research report deals with the results of the testing of Brusa motor used in electrical vehicles.

Keywords

Testing, permanent magnet synchronous machine

Contents

1 Introduction

This research report extends the research report 22190 – 027 – 2020 by the measurement of the Brusa HSM1-6.17.12 machine [1]. The Brusa HSM1-6.17.12 machine is mechanically coupled (back to back configuration) with the loading machine YASA P400RS [2] which has been modified to work under reduced dc-link voltage of 400V (reduced number of turns in the stator winding). A water cooled 3-phase voltage source inverter based on SIC switches is used to power the loading machine using 15kHz of the switching frequency (more about the converter can be found in [3]) .The actual test bad is in the Fig. 1 and in the context of the Brusa HSM1-6.17.12 machine measurement, it represents an equivalent setup as it was used in the research report [4]. The dc–links of both machines are connected. In the given test rig, the maximum speed is limited to 5500 rpm.

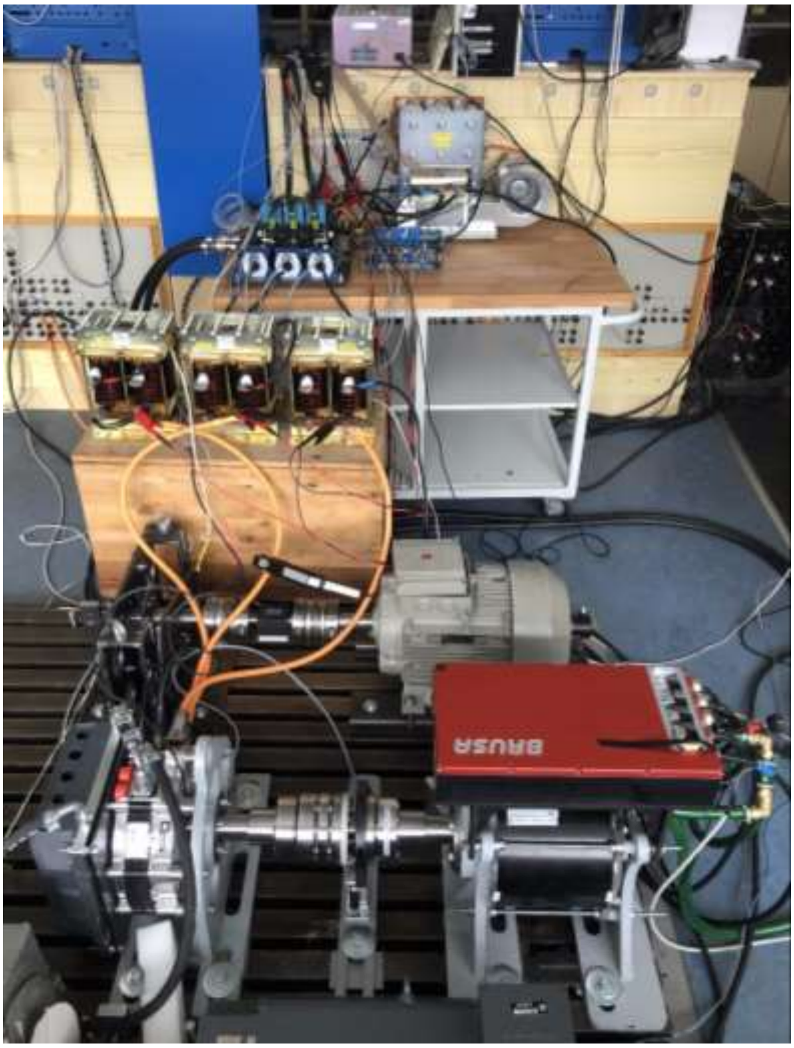

Fig. 1: Developed test rig for experiments on Brusa HSM1-6.17.12

The BRUSA HSM1-6.17.12 machine is powered by the 3-phase VSI Brusa DMC5 [3]. The parameters of the BRUSA HSM1-6.17.12 are shown in Table 1. and the parameters of the 3-phase VSI are in the Table 2.

Table 1: Motor parameters of the BRUSA HSM1-6.17.12 provided by the manufacturer [1]

Motor data	**BRUSA HSM1-6.17.12**	
DC voltage [V]	360 V	400 V
Nominal speed [rpm]	4700	5200
Continuous torque [Nm]	130	130
Max. torque [Nm]	220	220
Inverter current [Arms]	300	300
Continuous power [kW]	64	70
Maximum power [kW]	87	96
Maximum speed [rpm]	12000	12000
Level of efficiency [%]	95	
Number of pole pairs	3	
Number of turns	7	
Nominal frequency [Hz]	210	
Maximum frequency [Hz]	600	
Max. motor flux [Vs]	0.725	
Stator leakage inductance [µH]	47	
Stator resistance [mΩ]	20	

Table 2: Technical data of the inverter provided by the manufacture [3]

Technical data	**DMC534**
Min. HV input for operation [V]	130
Min. HV input for full electrical output [V]	200
Max. HV input [V]	450
Software disconnection [V]	460
Hardware disconnection [V]	480
Max HV input without damage [V]	520
Continuous output [kW]	118
Max. output [kW]	157
PWM frequency [kHz]	24

More detailed description of the drive together with measured parameters of the equivalent circuit can be found in [4].

2 Machine characteristics measurement under load conditions

The purpose of the experiment is to map the characteristics of BRUSA HSM1-6.17.12 machine across the operational range of speed and load conditions. The torque and power characteristics in dependency of speed and the efficiency map provided by the manufacturer are in Fig. 2 and in Fig. 3.

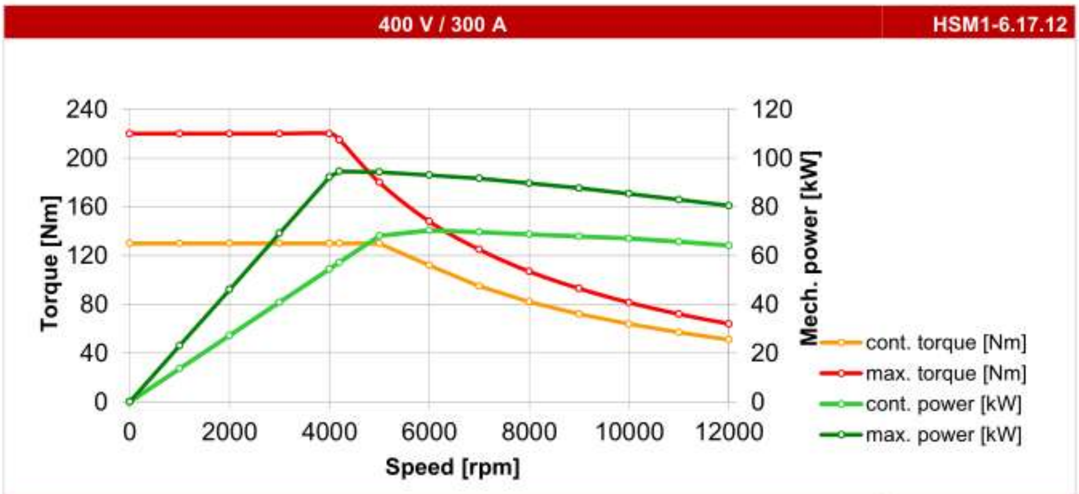

Fig. 2: Efficiency map of Brusa motor provided by the manufacturer [1]

400 V															HSM1-6.17.12
SPEED [RPM]	TORQUE [NM]														
	10	20	30	40	50	60	70	80	100	120	140	160	180	200	220
100	84,14	80,37	77,43	74,28	71,57	68,94	66,41	64,28	60,33	57,14	53,75	50,86	48,26	45,82	43,98
200	89,03	87,64	86,16	84,30	82,67	80,83	79,36	77,74	75,84	72,07	69,52	66,94	64,64	62,50	60,36
300	91,25	90,19	89,57	88,19	87,49	85,89	84,66	83,54	81,43	79,56	77,25	75,41	73,26	71,44	69,62
400	92,02	91,79	91,52	90,51	89,53	88,55	87,65	86,70	84,94	83,23	81,50	79,72	78,06	76,49	74,86
500	94,82	94,19	92,94	92,25	91,37	90,55	90,04	89,02	87,43	86,00	84,65	83,06	81,60	80,21	78,69
1000	94,24	95,65	95,23	94,90	94,56	94,18	93,88	93,48	92,57	91,92	91,02	90,19	89,28	88,40	87,60
2000	91,09	94,93	94,93	95,29	95,29	95,26	95,26	95,14	94,82	94,68	94,14	93,76	93,30	92,85	92,37
3000	91,32	93,96	95,00	95,26	95,61	95,63	95,76	95,69	95,62	95,44	95,23	94,90	94,66	94,27	93,97
3400	91,37	94,09	94,85	95,31	95,64	95,77	95,95	95,93	95,89	95,70	95,51	95,29	95,01	94,77	94,42
3600	91,02	93,81	94,55	95,23	95,40	95,69	95,81	95,88	95,87	95,76	95,57	95,31	95,07	94,79	94,52
3800	90,72	93,90	94,60	95,23	95,50	95,74	95,82	95,86	95,94	95,80	95,64	95,41	95,17	94,95	94,69
4000	90,82	93,69	94,70	95,11	95,50	95,68	95,93	95,92	95,84	95,90	95,61	95,45	95,25	95,08	94,70
4200	94,05	95,04	95,36	95,70	95,91	96,08	96,10	96,06	95,95	95,81	95,63	95,40	94,74	NaN	NaN
4400	91,85	94,17	94,81	95,37	95,67	95,88	96,17	96,00	96,05	95,98	95,89	95,69	95,31	NaN	NaN
4600	92,88	93,89	95,11	95,47	95,76	95,76	95,96	96,06	96,05	96,10	95,84	95,54	95,03	NaN	NaN
4800	91,08	94,24	94,82	95,31	95,79	95,92	96,07	96,09	96,16	95,99	95,69	95,22	94,56	NaN	NaN
5000	91,94	93,75	94,70	95,32	95,66	95,99	96,04	96,11	96,15	96,00	95,51	95,16	NaN	NaN	NaN
5200	91,21	93,61	94,65	95,26	95,82	95,88	96,11	96,06	96,09	95,82	95,43	94,78	NaN	NaN	NaN
6000	89,76	92,98	94,40	95,14	95,49	95,66	95,75	95,67	95,21	95,01	94,06	NaN	NaN	NaN	NaN
7000	89,03	93,19	94,76	95,07	95,18	95,26	95,28	94,99	94,44	93,02	NaN	NaN	NaN	NaN	NaN
8000	88,69	92,58	93,97	94,33	94,47	94,46	94,23	93,86	92,47	NaN	NaN	NaN	NaN	NaN	NaN
9000	88,14	91,93	93,07	93,18	93,64	93,43	92,97	92,42	91,48	NaN	NaN	NaN	NaN	NaN	NaN
10000	87,37	90,92	92,24	92,88	92,83	92,22	91,50	90,88	NaN	NaN	NaN	NaN	NaN	NaN	NaN
11000	84,53	89,20	91,19	91,49	91,73	87,77	90,11	NaN	NaN	NaN	NaN	NaN	NaN	NaN	NaN
12000	84,56	89,01	90,44	90,63	90,53	89,42	88,80	NaN	NaN	NaN	NaN	NaN	NaN	NaN	NaN

Fig. 3: Efficiency map of Brusa motor provided by the manufacturer [1]

The measured speed range was limited to 5500 rpm due to physical limitation of the test rig. The particular operation points were measured in the range of the speed $n \in \langle 500, 5500 \rangle$ rpm with a step of 500 [rpm] each for various values of the load torque in the range of $T_L \in \langle 0, 155 \rangle$ [Nm]. The DC-link voltage was V_{dc}= 400 V. The power on the shaft is obtained by measurement of the load torque, which is measured by the torque sensor T40B [6] with the measurement range of $T \in \langle -500, 500 \rangle$ [Nm]. The data are collected by the module TIM 40 [6], and then sent to the oscilloscope as an analogue voltage value in the range of ±10 V as shown in Fig. 5.

For each operational point we have measured two phase currents and two phase to phase voltages together with mechanical speed n and load torque T_L. A typical measured waveform is shown in Fig. 4.

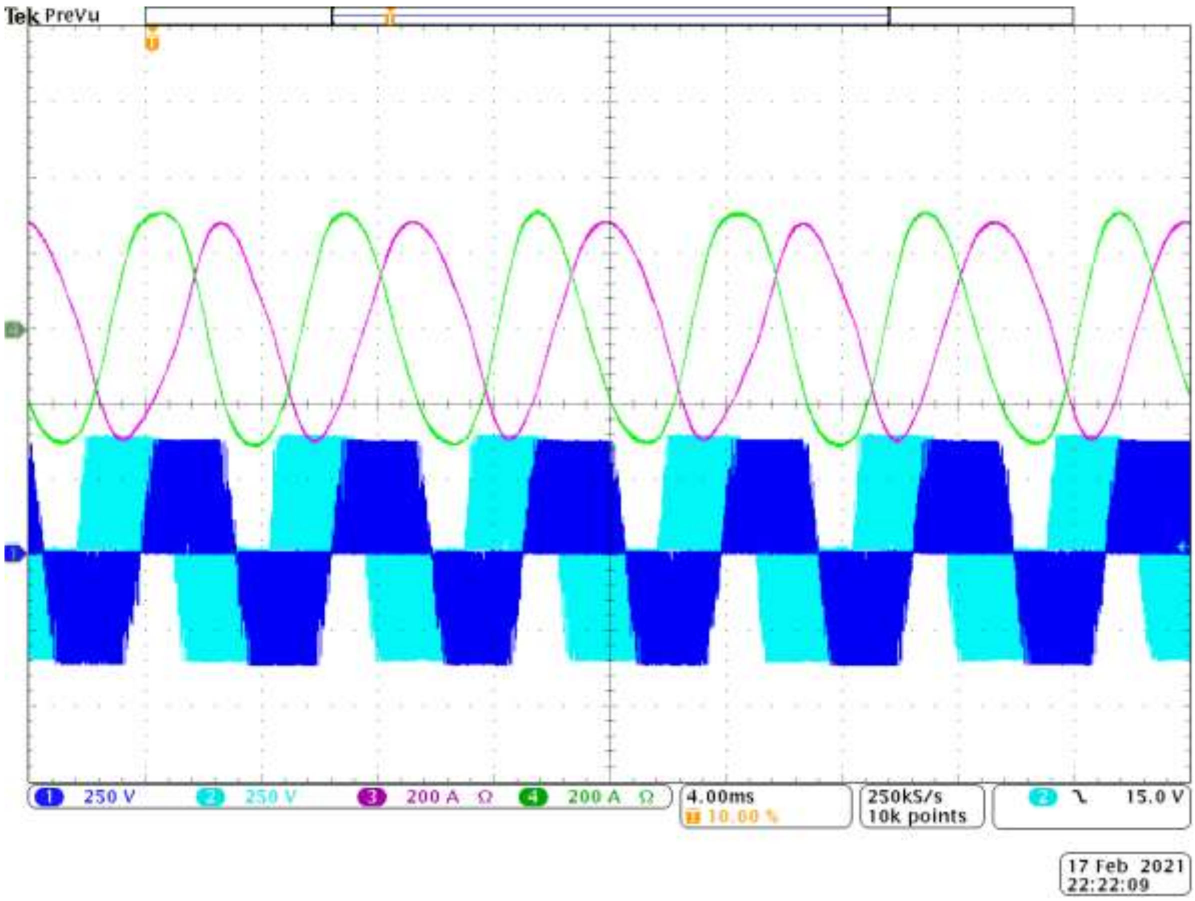

Fig. 4: Typical waveforms of measured phase currents and phase to phase voltages, where CH 3 (purple) is phase current I_{sv} [200A/div] CH 4 (green) is phase current I_{su} [200A/div] CH1 (dark blue) is phase to phase voltage V_{vw} [250V/div] and CH2 (light blue) is line voltage V_{uv} [250V/div]. Mechanical speed n = 300rpm and stator temperature is 41°C

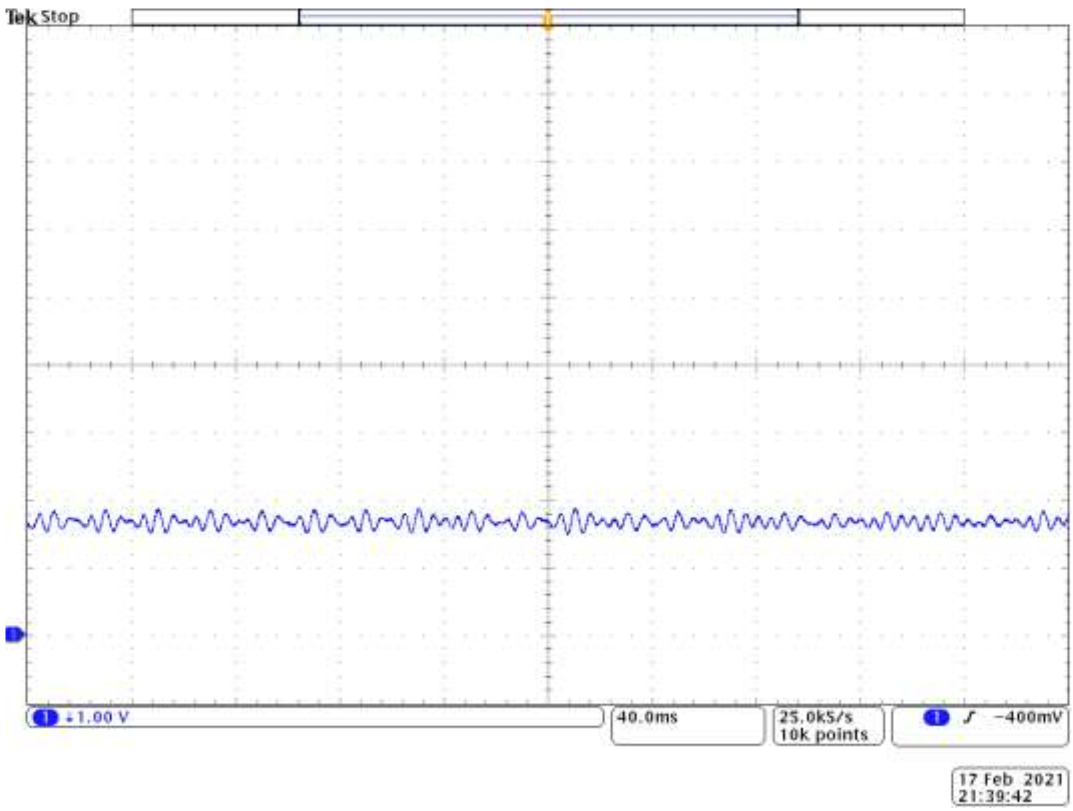

Fig. 5: Load torque measurement corresponding to Fig. 4: CH1 is load torque TL [50Nm/div]

From the measured currents and voltages, we reconstruct the phase currents and voltages in each phase of the machine as it is illustrated in Fig. 6 and Fig. 7.

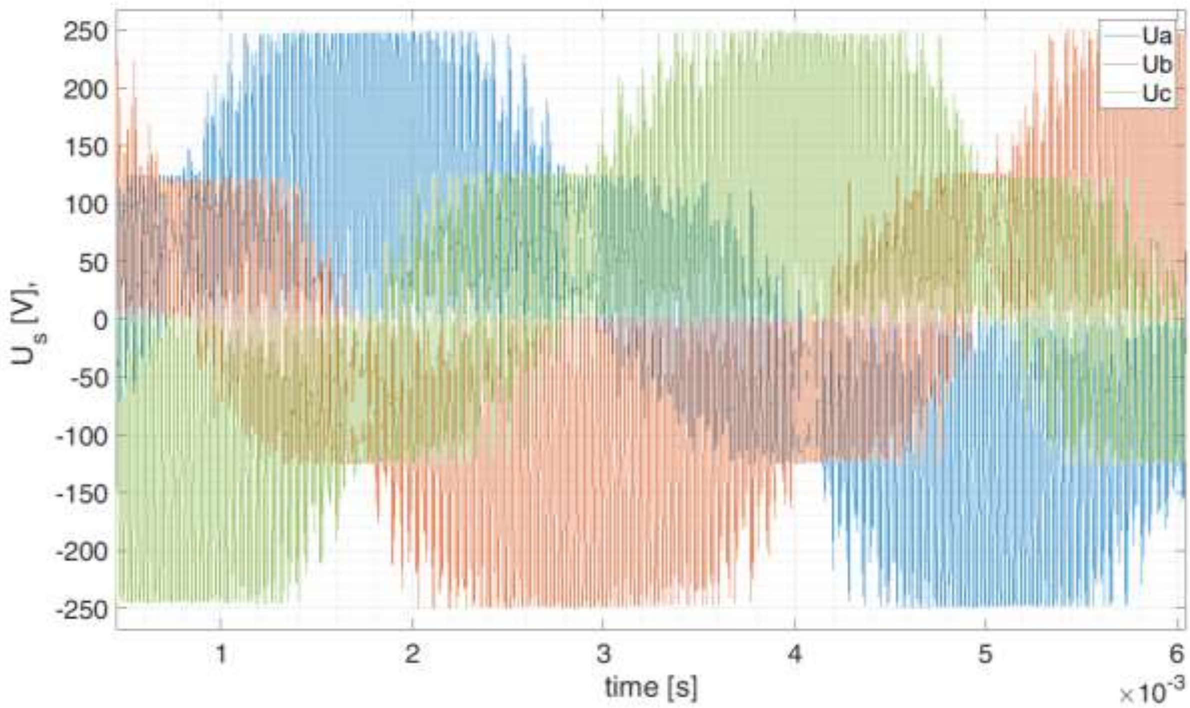

Fig. 6: Waveforms of reconstructed phase voltages U_s [V]

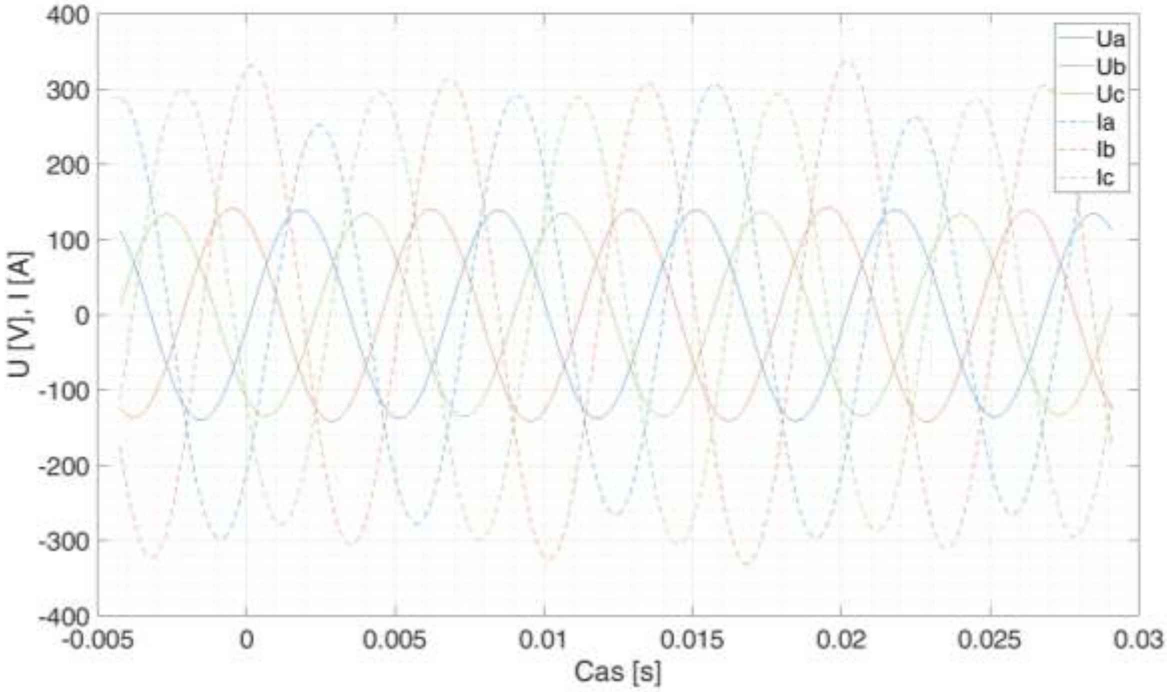

Fig. 7: Waveforms of reconstructed phase voltages U_s (filtered) [V] and phase currents I_s [A].

The amplitudes and their phases of the phase currents I_s and phase voltages U_s are obtained by the FFT analysis (see Fig. 8 and Fig. 9).

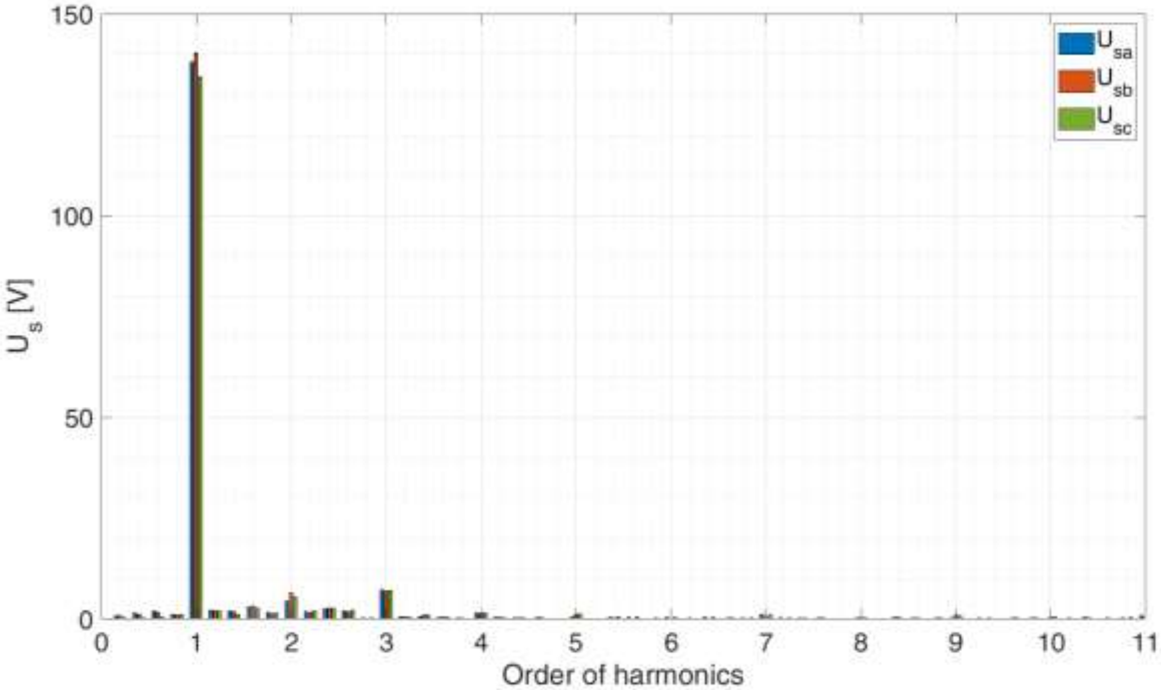

Fig. 8: FFT of the phase voltage U_s from Fig. 7

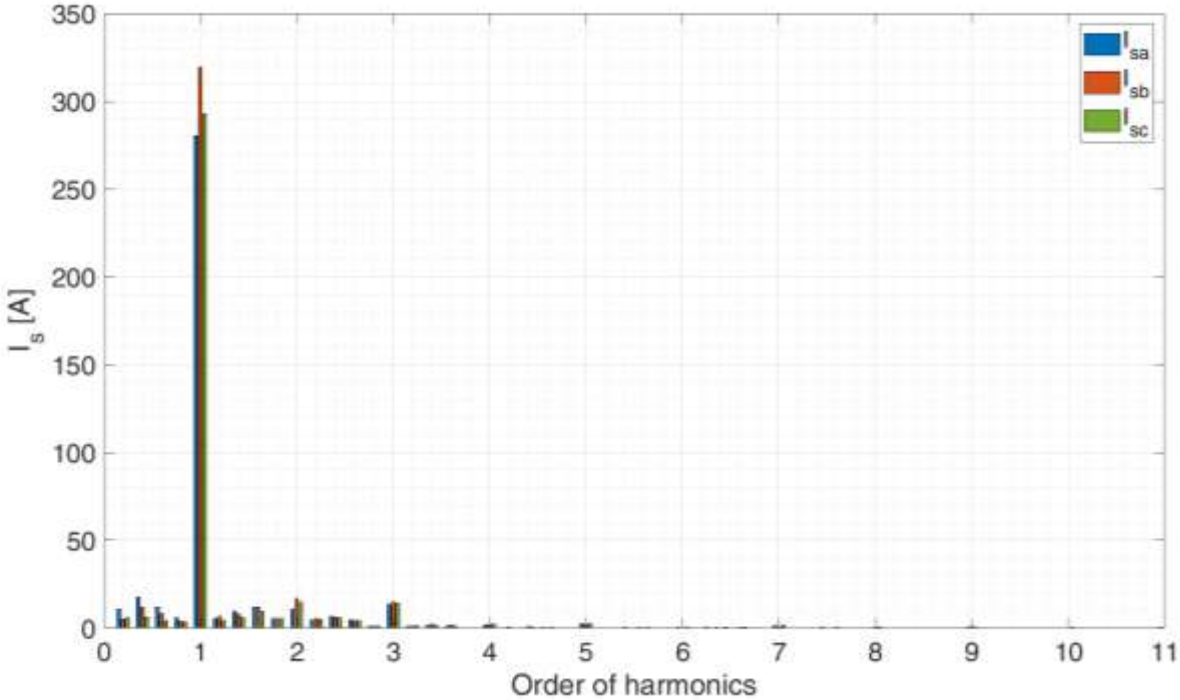

Fig. 9: FFT of the phase current I_s from Fig. 7

The complex power $\boldsymbol{S}$ for each harmonics μ can be found as

$$\boldsymbol{S_\mu} = \frac{1}{2}\boldsymbol{U_\mu I_\mu^*} = \frac{1}{2}U_\mu e^{j\varphi_{U_\mu}} \cdot I_\mu e^{-j\varphi_{I_\mu}} = \frac{1}{2}U_\mu I_\mu e^{j\left(\varphi_{U_\mu}-\varphi_{I_\mu}\right)} = \frac{1}{2}U_\mu I_\mu e^{j\varphi_\mu} \qquad (2.1)$$

The real component of the power *P* for specific harmonics is than

$$P_\mu = \mathfrak{R}\{\boldsymbol{S_\mu}\} = \frac{1}{2}U_\mu I_\mu \cos\varphi_\mu \qquad (2.2)$$

The overall power is than computed as

$$P_{el} = \mathfrak{R}\{\boldsymbol{S}\} = \sum_{\mu=1}^{N} \frac{1}{2}U_\mu I_\mu \cos\varphi_\mu, \qquad (2.3)$$

Where N is the number of investigated order of harmonics.

$$\eta = \frac{P_{mech}}{P_{el}} \qquad (4.4)$$

Where the P_{mech} is mechanical power on the shaft which is obtain from

$$P_{mech} = T\omega \qquad (4.5)$$

Here, $\omega = rpm\frac{2\pi}{60}$, is the measured mechanical angular speed and T_m is the measured torque. Note that the same method of machine efficiency evaluation has been used in [4].

The machine has been analyzed for all selected operational points and the result is provided in the efficiency map of the machine. Specifically, Fig. 10 shows the dependency of the efficiency η on mechanical speed n and torque measured on the shaft T. And the Fig. 11 shows the dependency of the machine efficiency η on mechanical speed n and stator current I_s. The efficiency maps reconstructed using only first harmonics are shown in the Fig. 12 and Fig. 13. Fig. 14 and Fig. 15 show electrical power depending on mechanical speed and electromagnetic torque. Fig. 16 shows the same graph for mechanical power P_{mech}.

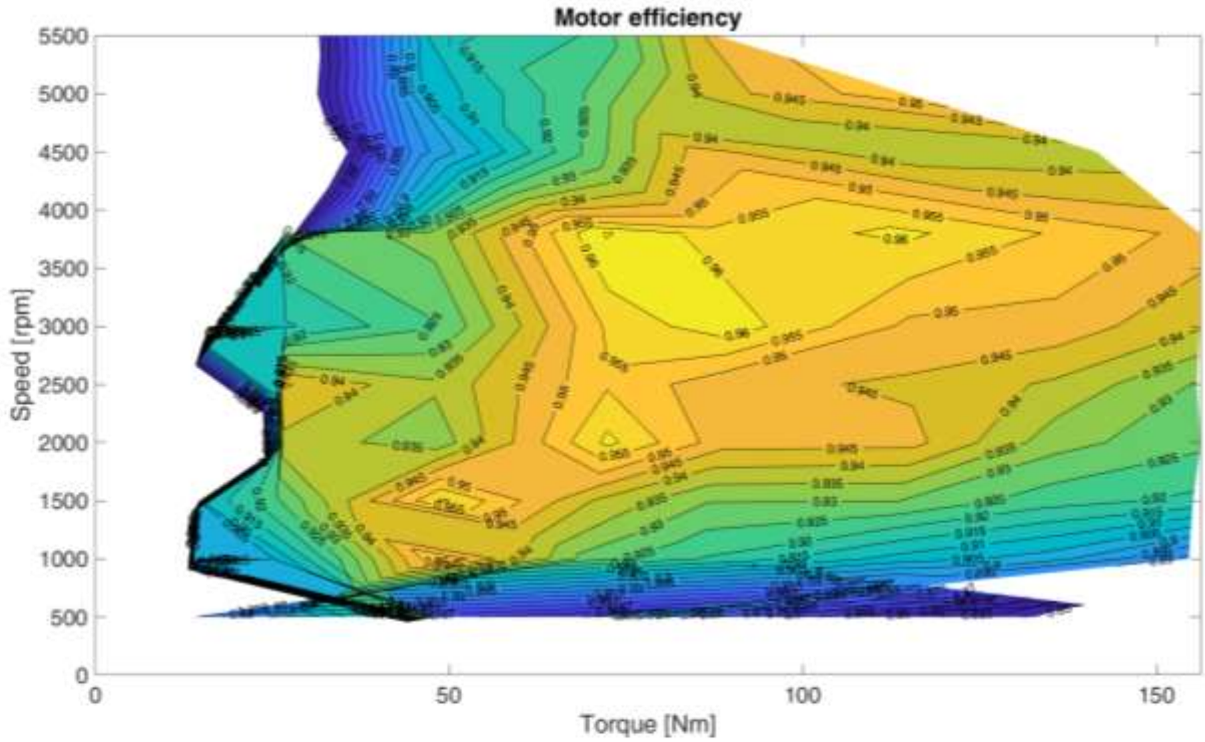

Fig. 10: Machine efficiency η depending on torque and speed

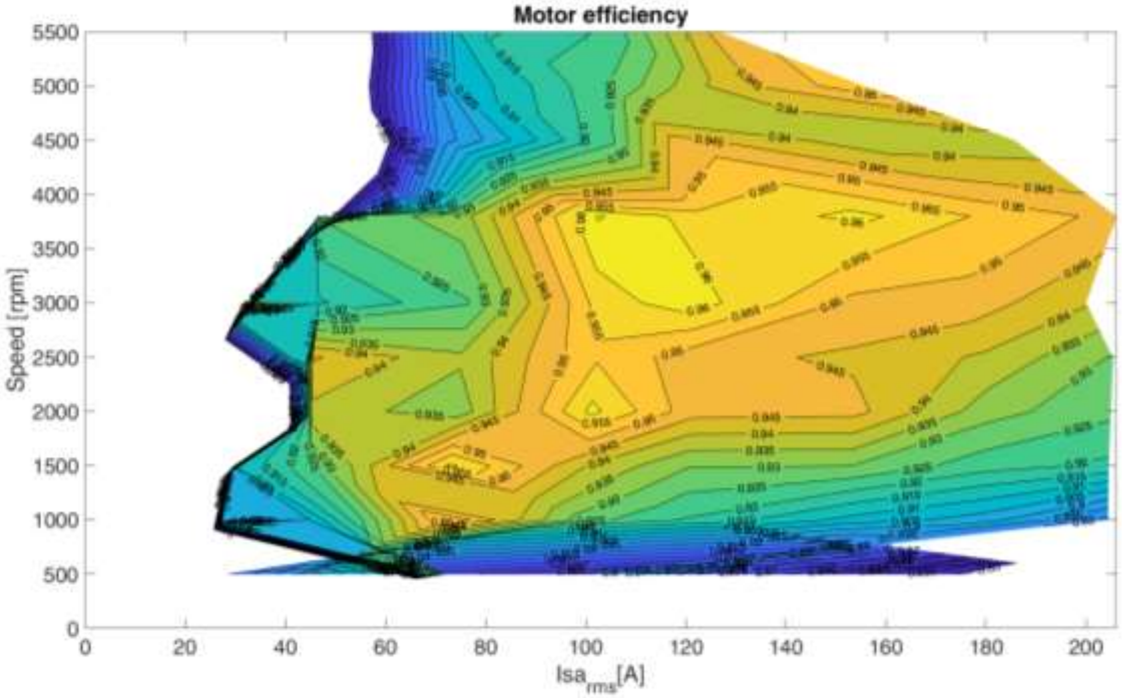

Fig. 11: Machine efficiency η depending on the mechanical speed n [rms] and the stator current I_s [A]

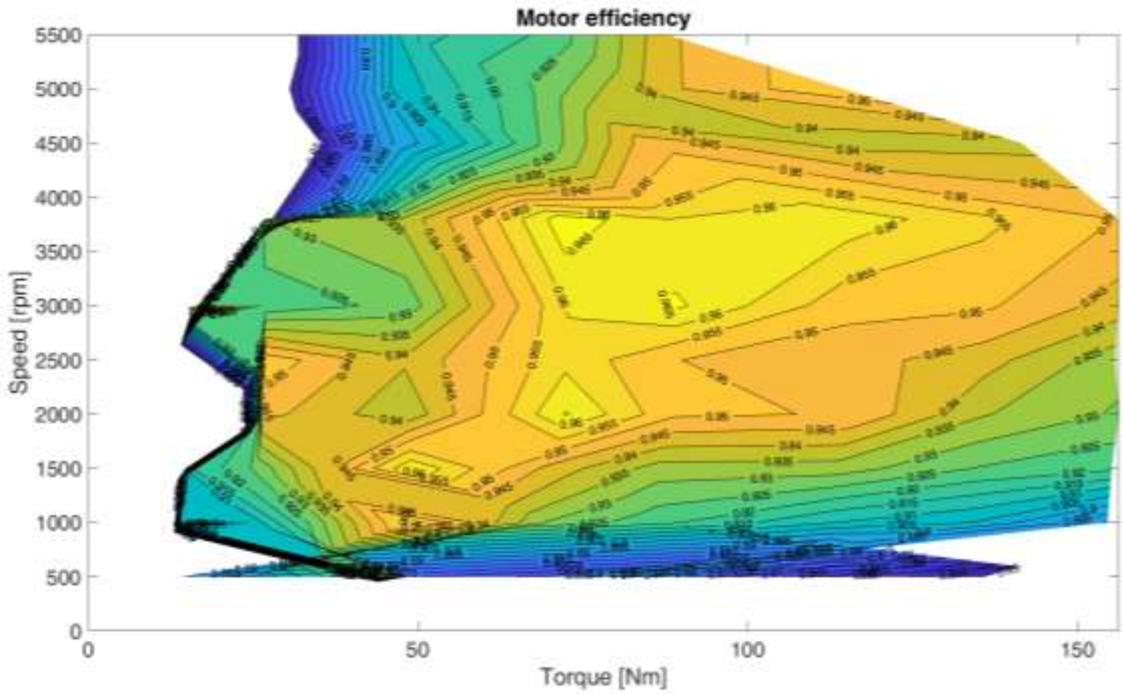

Fig. 12: Machine efficiency η_1 depending on torque and speed

Since higher order harmonics increase overall losses, we illustrate the efficiency of the machine powered by harmonic signals by calculating η_1 which is obtained using only first harmonics as

$$\eta_1 = \frac{P_{mech}}{P_{el(1)}} \quad (4.6)$$

$$P_{el(1)} = \frac{1}{2} U_1 I_1 \cos \varphi_1, \tag{2.7}$$

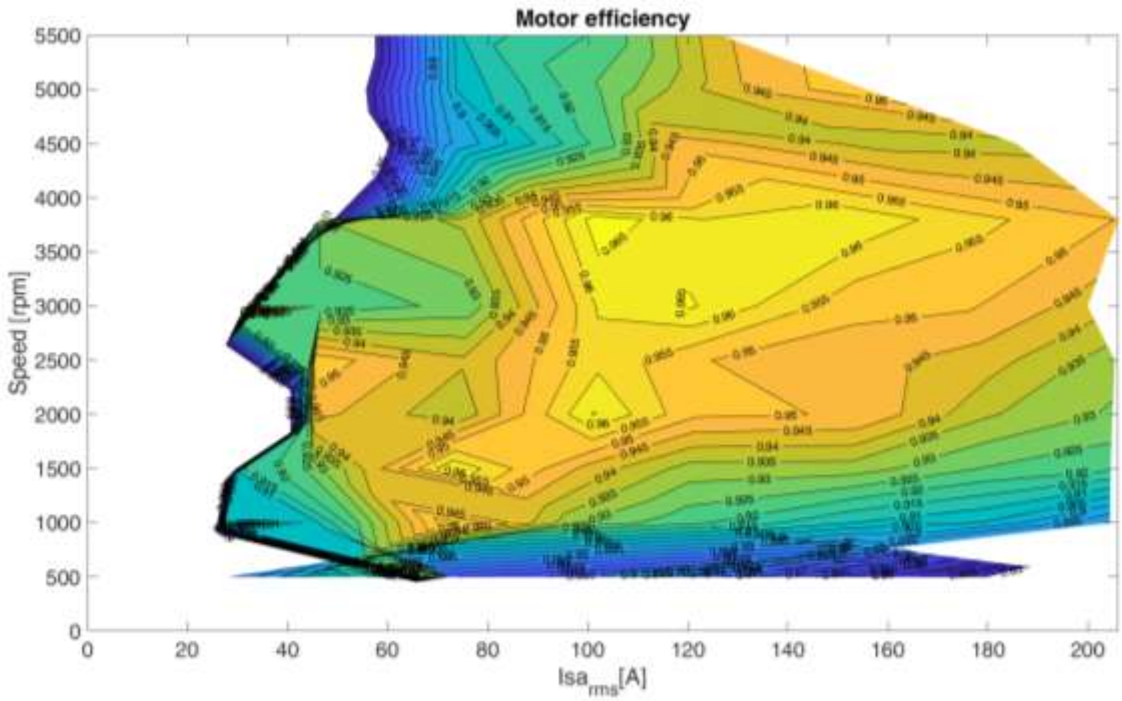

Fig. 13: Machine efficiency η_1 depending on the mechanical speed n [rms] and the stator current I_s [A]

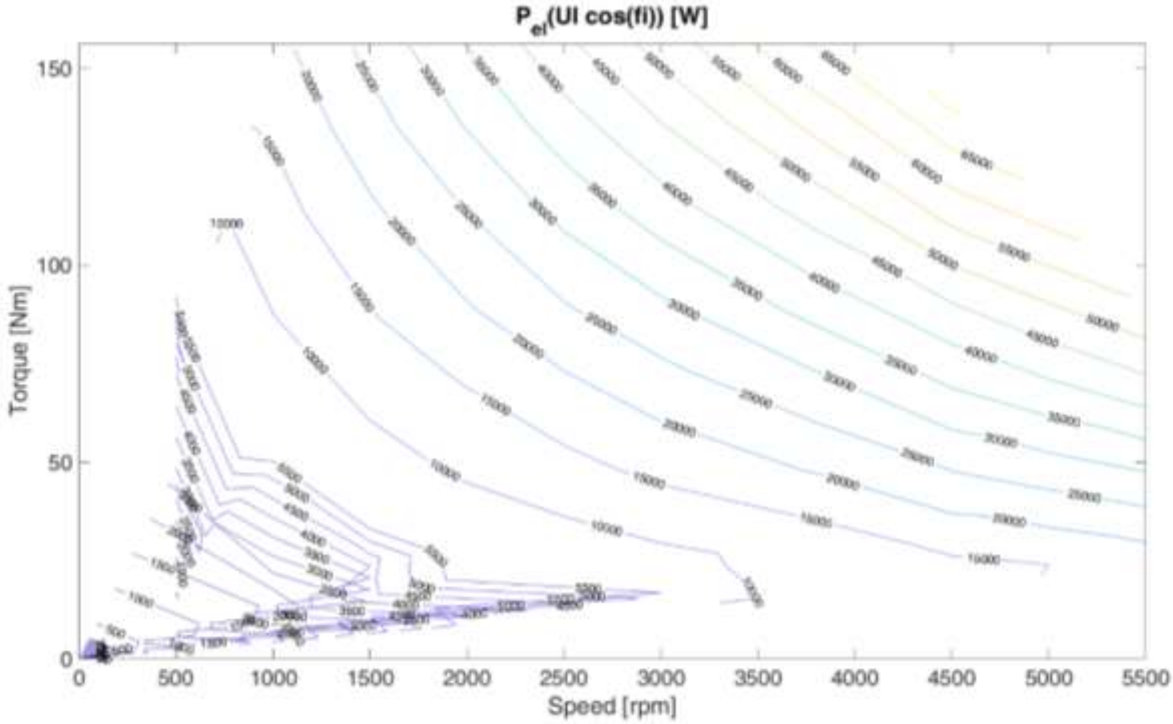

Fig. 14: Electrical power $P_{el(1)}$ (note that only first harmonic is involved in computation of $P_{el(1)}$, see (4.7)) depending on the mechanical speed n [rms] and torque T [Nm].

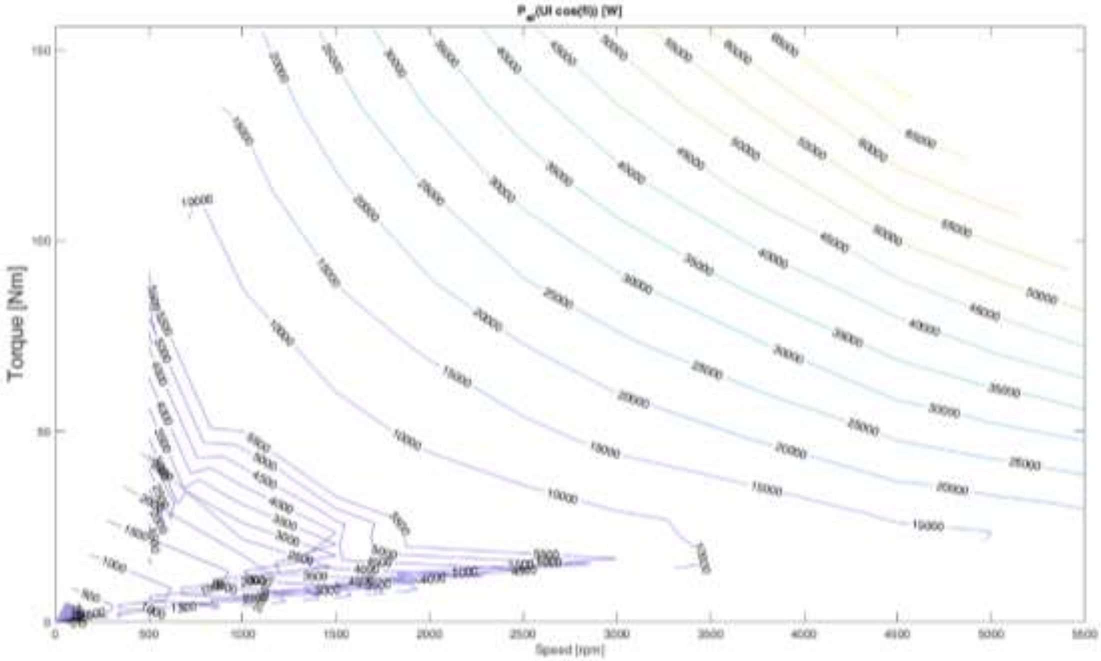

Fig. 15: Electrical power P_{el} (see (4.3)) depending on the mechanical speed n [rms] and torque T [Nm].

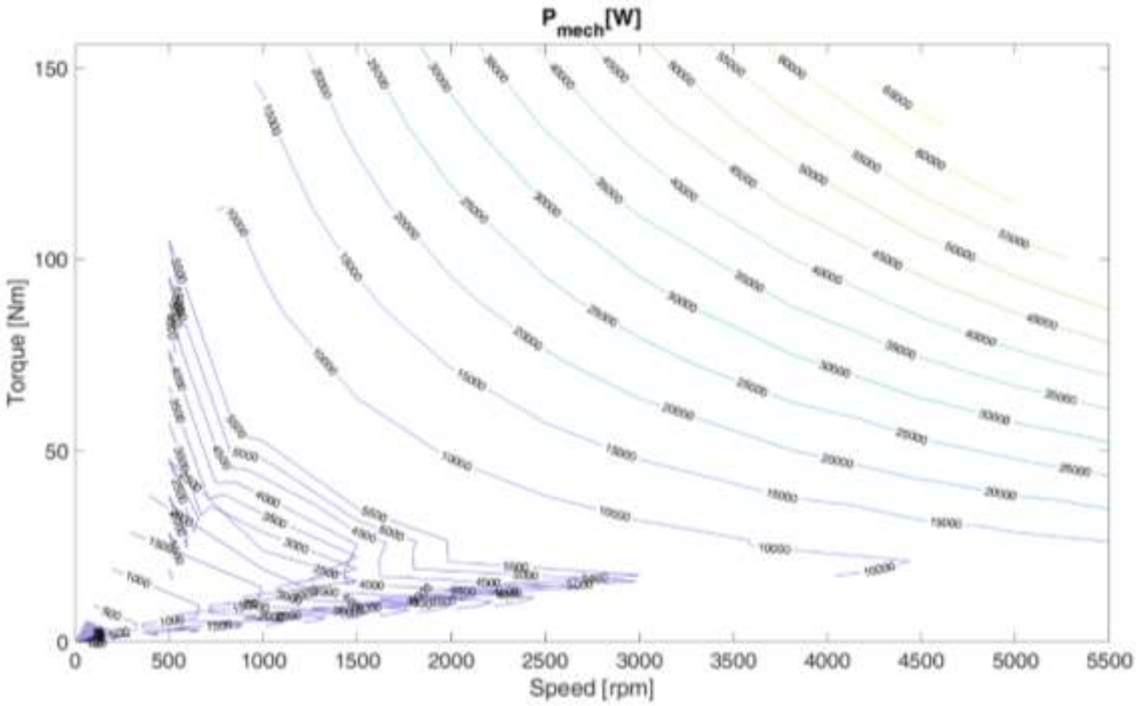

Fig. 16: Mechanical power P_{mech} depending on the mechanical speed n [rms] and torque T [Nm].

3 Conclusion

This research report extends the results of the research report [4]. The main goal is to analyse the efficiency of Brusa HSM1-6.17.12 machine in the wide spectrum of operational points. The machine characteristics are measured up to the rotor speed of 5500 rpm. The resulting characteristics of the machine approximately comply with the values provided by Brusa Company. The deviations in the low speed region and low load torque regions may be caused by the high noise/measured value ratio. Additionally, the mechanical resonances of the test rig appearing at n=2150-2400 [rpm] and n=4800-5000 [rpm] may further disrupt the results. In order to illustrate the efficiency of the machine powered by pure harmonic signal, we provide the efficiency maps using reconstructed only first harmonics of U and I – those results are shown in Fig. 12 and Fig. 13.

References

[1] Brusa HSM1-6.17.12. *Brusa Elektronik AG*. [online]. [cit. 5.5.2020] Available from: https://www.brusa.biz/en/products/drive/motor-400-v/hsm1-61712.html

[2] YASA P400R Series. *YASA Limited*. [online]. [cit. 5.5.2020] Available from: https://www.yasa.com/yasa-p400/

[3] ŠTĚPÁNEK, Jan, Pavel DRÁBEK and Jiří OČENÁŠEK. Wide bandgap devices based main traction converter with high power density: 22190-FV028-2020. Západočeská univerzita v Plzni, 2020.

[4] LAKSAR, Jan, Zdeněk FRANK, Štěpán JANOUŠ, Ondřej SUCHÝ, Martin ŠESTÁK, Jan ŠTĚPÁNEK and Tomáš KOMRSKA. Analysis of the axial flux electromotor for the electric vehicles and P1 hybrid electric vehicles: 22190–027–2020. Západočeská univerzita v Plzni, 2020.

[5] Brusa DMC5_Manual_EN. *Brusa Elektronik AG*. [online]. [cit. 5.5.2020] Available from: https://www.brusa.biz/portfolio/dmc534/

[6] T40B torque sensor. *HBP measurement technology*. [online]. [cit. 26.5.2020] Available from: https://www.hbm.cz/produkty/snimace-krouticiho-momentu/t40b/

List of Figures

Revision history

Rev.	Chapter	Description of change	Date	Name
0	All	Document release	11.3.2021	O.Suchý